Article

Electrostatic Potential Field Effects on Amine Macrocyclizations within Yoctoliter Spaces: Supramolecular Electron Withdrawing/ Donating Groups

Published as part of The Journal of Physical Chemistry virtual special issue "Dor Ben-Amotz Festschrift".

Wei Yao, Kaiyu Wang, Yahya A. Ismaiel, Ruiqing Wang, Xiaoyang Cai, Mary Teeler, and Bruce C. Gibb*

Read Online

ACCESS | 📊 Metrics & More | 📰 Article Recommendations | 🆂🅸 Supporting Information

ABSTRACT: The central role of Coulombic interactions in enzyme catalysis has inspired multiple approaches to sculpting electrostatic potential fields (EPFs) for controlling chemical reactivity, including ion gradients in water microdroplets, the tips of STMs, and precisely engineered crystals. These are powerful tools because EPFs can affect all reactions, even those whose mechanisms do not involve formal charges. For some time now, supramolecular chemists have become increasingly proficient in using encapsulation to control stoichiometric and catalytic reactions. However, the field has not taken advantage of the broad range of nanocontainers available to systematically explore how EPFs can affect reactions within their inner-spaces. With that idea in mind, previously, we reported on how positively and negatively charged supramolecular capsules can modulate the acidity and reactivity of thiol guests bound within their inner, yoctoliter spaces (Cai, X.; Kataria, R.; Gibb, B. C. *J. Am. Chem. Soc.* **2020**, *142*, 8291−8298; Wang, K.; Cai, X.; Yao, W.; Tang, D.; Kataria, R.; Ashbaugh, H. S.; Byers, L. D.; Gibb, B. C. *J. Am. Chem. Soc.* **2019**, *141*, 6740−6747). Building on this, we report here on the cyclization of 14-bromotetradecan-1-amine inside these yoctoliter containers. We examine the rate and activation thermodynamics of cyclization (Eyring analysis), both in the absence and presence of exogenous salts whose complementary ion can bind to the outside of the capsule and hence attenuate its EPF. We find the cyclization rates and activation thermodynamics in the two capsules to be similar, but that for either capsule attenuation of the EPF slows the reaction down considerably. We conclude the capsules behave in a manner akin to covalently attached electron donating/withdrawing groups in a substrate, with each capsule enforcing their own deviations from the idealized S_N2 mechanism by moving electron density and charge in the activated complex and TS, and that the idealized S_N2 mechanism inside the theoretical neutral host is relatively difficult because of the lack of solvation of the TS.
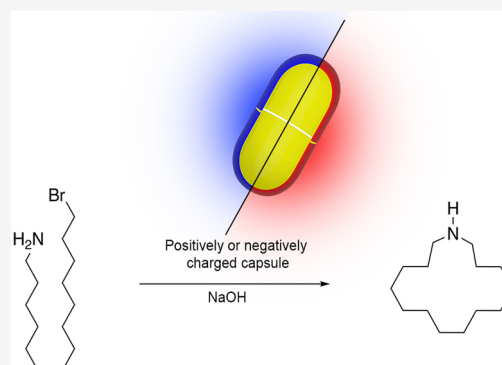
INTRODUCTION

Inspired by the strength and long range of Coulombic interactions and their central role in the properties of enzymes,[1−6] multiple approaches for controlling chemical reactions by sculpting electrostatic potential fields (EPFs) have been considered.[7] Examples include utilizing the concentration gradients and the resulting EPF gradients in water micro-droplets,[8] using the intense EPFs of STM tips,[9−12] or employing crystal engineering to sculpt EPFs within crystals.[13,14] These represent powerful potential tools for chemists; even reactions whose mechanisms do not involve formal charges, e.g., the classic Diels−Alder reaction, can be accelerated by external EPFs because many formally covalent species along the reaction pathway are stabilized by minor charge-separated resonance contributors that are themselves affected by the applied field.[9,15]

One of the first examples of solution-based control of EPFs in reactions utilized diethyl ether solutions of 5 M LiClO₄ and took advantage of the dissimilar coordination (supramolecular) properties of Li⁺ and ClO₄⁻ ions.[16] Since that time, although supramolecular chemistry has become increasingly proficient in using encapsulation to control stoichiometric and catalytic reactions,[17−36] the field has not taken advantage of the broad range of nanocontainers available to systematically explore how EPFs can affect reactions within their inner-spaces.[37]
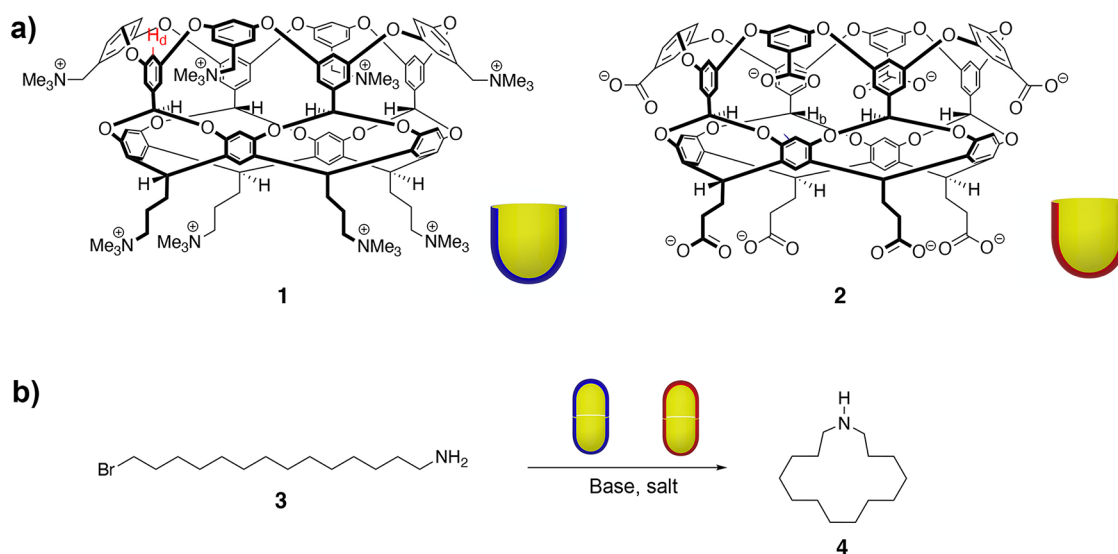
Figure 1. (a) Hosts utilized in this study: positand **1** and octa-acid (carboxylate) **2**. Also shown are schematic representations of the hosts as, respectively, blue and red bowls. (b) Cyclization of 14-bromotetradecan-1-amine **3** inside capsules **1**$_2$ and **2**$_2$ to give azacyclopentadecane **4**.

As a step toward understanding how the EPFs of hosts can affect the reactions of internalized guests, we recently reported on two, oppositely charged, yoctoliter containers built from positand **1** and octa-acid **2** (Figure 1).[38−40] Through the hydrophobic effect, these cavitands dimerize around guests to form container complexes possessing identically shaped, low dielectric inner-spaces that differ in one key point; namely, the yoctoliter inner-spaces of **1**$_2$ and **2**$_2$ are, respectively, enveloped in a positive and negative EPF generated by the water-solubilizing charged groups of each cavitand. How does this difference affect chemical reactivity? We have shown that bound thiol guests are more acidic inside **1**$_2$, by up to 2.5 pK_a units (it transpires that guest motif has a much larger effect on pK_a).[41] We have also observed that rates of macrocyclization of α,ω-thio-alkane halides inside **1**$_2$ are almost 4 orders of magnitude faster than inside **2**$_2$.[42] These findings also showed that the stabilization of the transition states (TS) for cyclization was greater than that of thiolate stabilization, suggesting a rather complex mechanism by which these capsules affect chemical reactivity.

To extend our understanding of these yoctoliter reaction flasks further, we report here on the cyclization of 14-bromotetradecan-1-amine (**3**, Figure 1) inside yoctoliter containers **1**$_2$ and **2**$_2$. We examine the rate of formation of azacyclopentadecane (**4**), both in the presence of a minimum amount of exogenous salt, as well as in the presence of excesses of a range of different salts to examine how capsule counterion changes affect its EPF and hence the rate of cyclization within. We also perform Eyring analysis in the absence and presence of selected salts to determine the activation thermodynamics and how these are affected by exogenous salt binding. Overall, we find the cyclization rates and activation thermodynamics to be relatively insensitive to the nature of the EPF (**1**$_2$ versus **2**$_2$), but that for either capsule attenuation of the EPF slows the reaction down considerably. We conclude the capsules behave in a manner akin to electron donating/withdrawing groups covalently attached to the reaction center of **3**, with each capsule enforcing their own deviations from the idealized S$_N$2 mechanism by moving electron density and charge in the activated complex and TS. Additionally, we conclude that the

idealized S$_N$2 mechanism inside the theoretical neutral host is relatively difficult because of the lack of solvation of the TS.

■ RESULTS AND DISCUSSION

Host and Guest Synthesis, and Complex Formation. Cavitands **1** and **2** were formed using previously described procedures.[38−40] Guest **3** was synthesized via a four-step process from the corresponding diacid: double reduction (BH$_3$-Me$_2$S/B(OMe)$_3$) and bromination (NBS), followed by monoamination (phthalimide/K$_2$CO$_3$, then AcOH/HBr). Full details are given in the Supporting Information (SI, Section 2).

Solutions of **1** and **2** were formed by dissolving the material in D$_2$O containing a small excess of NaOD. The capsular complexes with the two hosts were then formed by the addition of a slight excess of half an equivalent of guest **3**·HBr in D$_2$O (SI Section 3). Figures S5−S12 show the ^{1}H NMR, DOSY NMR, and COSY NMR spectra of the two complexes. The ^{1}H NMR signals of guest **3** in the free (in D$_2$O) and encapsulated states were used to calculate the $\Delta\delta$ values for each signal. It is well-established that, because of the D_{4h} point group of the inner-space (approximately a spheroid or ellipsoid of revolution), the $\Delta\delta$ value of a group is reflective of its average location within the inner-space; as a rule of thumb, the closer a group is to a pole, the more its signal is upfield shifted because of its inevitable proximity to one or more aromatic rings.[43] Hence, with 16 atoms in the chain, we anticipated that a $\Delta\delta$ value analysis would reveal that in both capsules the guest adopt a U- or J-motif.[21,44−49] This was indeed the case, but despite the two inner-spaces being identical in shape, the guest adopted a slightly different motif within the two hosts (Figure 2, and SI Figures S8 and S12). The $\Delta\delta$ values for guest **3** within **1**$_2$ suggest an average motif in which four contiguous carbons at the amine terminus are all located deep in one polar region, the section of the mainchain around C-9 is located at the equator, and the halide terminus is deep within the opposing polar region of the capsule. In contrast, within **2**$_2$ the guest adopts a more distinct J-shaped motif in which the C-6/C-7 region of the guest is a turn located in one polar region of the capsule, the halide terminus occupies the other, and the amino group/ammonium is located at the equator.
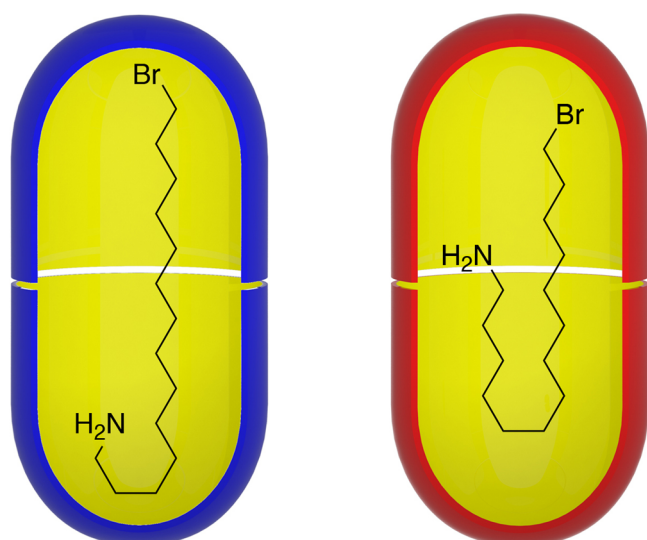
Figure 2. Representations of the average motif of guest 14-bromotetradecan-1-amine (**3**) inside capsules **1**$_2$ and **2**$_2$.

Three principal factors likely contribute to the subtle difference in average conformation of the guest in the two capsules. First, it may be the case that the hemispheres of capsule **1**$_2$ are slightly further apart than in **2**$_2$; the solubilizing groups of the former are more weakly solvated than the carboxylates of the latter,[50] and hence, the Coulombic repulsion between the hemispheres of **1**$_2$ is likely higher. This would lead to a slightly greater inner-space volume in **1**$_2$. Second, the different motifs may arise from the different ion−dipole interactions between the positively charged solubilizing groups of **1**$_2$ or the negatively charged groups of **2**$_2$, and the two terminal dipoles (CH$_2$→Br and CH$_2$→NH$_2$) of the guest. Prior modeling suggests a reasonably homogeneous EPF within each yoctoliter space,[42] but it may be the case that the intrinsic asymmetry of the different ion−dipole interactions, combined with small gradients within each, alters the preferred motif of the guest. Finally, differences in the pK_a of the bound guest may be the cause of the motif changes. Although it was not possible to observe the ^{1}H NMR signal for a −NH$_2$ or −NH$_3{}^+$ group of the bound guest, and therefore not possible to use ^{1}H NMR spectroscopy to determine ammonium pK_a values, we can use the previously determined pK_a values for thiols within **1**$_2$, and **2**$_2$ as a guide.[41] This data suggests that the pK_a of a bound ammonium can range from 6 to 12; the amine would be a weak base inside **1**$_2$, and a relatively strong base inside **2**$_2$. That trace protonation of the guest inside **2**$_2$ is a possibility that was suggested by a small change in the guest binding region of the ^{1}H NMR spectrum of the complex when an additional 50 equiv of NaOD was added. However, this change did not itself discernably change the overall guest binding motif. In short, our evidence to date suggests that changes in pK_a may play somewhat of a role in the differences in guest motif in the two capsules, but that other possibilities (capsule volume differences or changes in ion-dipole interactions between capsule and guest) cannot be excluded.

Cyclization of Guest 3 in the Absence of Excess Salt. Cavitands are now well-established agents for inducing cyclization reactions,[21,42,51−53] and heating of either complex led to a quantitative yield of azacyclopentadecane **4**. There was no evidence of side reactions such as elimination or hydrolysis, nor polymer formation; this latter point confirms that

cyclization occurred exclusively within the inner-spaces of the capsules. To gather information about these cyclization reactions, we performed Eyring analyses using ^{1}H NMR spectroscopy (SI, Section 4).[54] In these experiments, the H$_d$ proton of each cavitand (Figure 1, highlighted in red in **1**) proved to be a useful reporter to monitor product formation. Thus, we determined the cyclization rate constants at five different temperatures for each complex. In the case of the cyclization of **3** within **1**$_2$, the reaction was monitored between 339 and 351 K, while in the case of the reaction inside **2**$_2$ the temperature range was 325−338 K. The obtained thermodynamic data shown in Table 1 reveals that the $\Delta H^{\ddagger}$ for

Table 1. Eyring Data for the Cyclization of Guest 3 within Capsules 1$_2$ and 2$_2$[a]

	3 in 1$_2$	3 in 2$_2$
k (s^{-1}, 338 K)	3.47×10^{-5}	6.25×10^{-5}
k (s^{-1}, 298.15 K)	1.77×10^{-6}	1.58×10^{-6}
half-life (s, 338 K)[a]	2.00×10^4	1.10×10^4
half-life (s, 298.15 K)[a]	3.90×10^5	4.38×10^5
$\Delta G^{\ddagger}$ (kJ mol^{-1})	105.8	106.2
$\Delta H^{\ddagger}$ (kJ mol^{-1})	59.8	74.5
$-T\Delta S^{\ddagger}$ (kJ mol^{-1})	45.9	31.7

[a]Errors in individual rate constant determinations <10%. Error in Eyring analysis ($\Delta G^{\ddagger}$, $-\Delta H^{\ddagger}$, $T\Delta S^{\ddagger}$) 5%.

cyclization is considerably lower within **1**$_2$ than within **2**$_2$ ($\Delta\Delta H^{\ddagger}$ = 14.7 kJ mol^{-1}). Interestingly, this difference is smaller than that seen in the cyclization of thiolates within the two capsules ($\Delta\Delta H^{\ddagger}$ = 24.3 kJ mol^{-1}), suggesting that the difference in charge development in the TSs for the formation of **4** inside **1**$_2$ versus inside **2**$_2$ is quite small. Although the reaction within **1**$_2$ possesses a lower enthalpy barrier, cyclization is more entropically penalized. One possible cause for this difference in $-T\Delta S^{\ddagger}$ is the location of the two termini of the guest in each complex (Figure 2); the greater average distance between the termini of the guest in the **1**$_2$ capsule would result in a higher entropic penalty to reach the TS. Because of these noted enthalpy and entropy differences, in the two capsules the reaction free energies of activation, rate constant, and half-life are not significantly different.

As we have not observed encapsulation to shift pK_a values of ionizable guests by more than 6 units, mechanistically we envision the S$_N$2 cyclization of **3** to involve the free amine; there is no amide ion formation since in the most favorable situation (inside positively charged **1**$_2$) the pK_a of an amine is unlikely to be below 30−32. Assuming an amine nucleophile, how do the capsules affect the mechanism? One way to envisage the effects of the EPF of the two capsules is by a More O'Ferrall−Jencks diagram (Figure 3), i.e., a plan projection of a reaction energy surface.[55,56] In the following discussion, we assume that the stabilization of the (partially) charged carbon center is energetically key, because its relatively high instability is disproportionally affected by the EPF of the capsule. In Figure 3, the black diagonal from top left to bottom right corresponds to the reaction coordinate of the idealized S$_N$2 mechanism from **3** to **4**, the left and lower axes correspond to the reaction coordinate of the idealized S$_N$1 mechanism, and the top and right axes correspond to the reaction coordinate of an addition−elimination process involving a pentavalent carbanionic TS.[57,58] The transition state for the S$_N$2 mechanism (●) occurs relatively early in the reaction
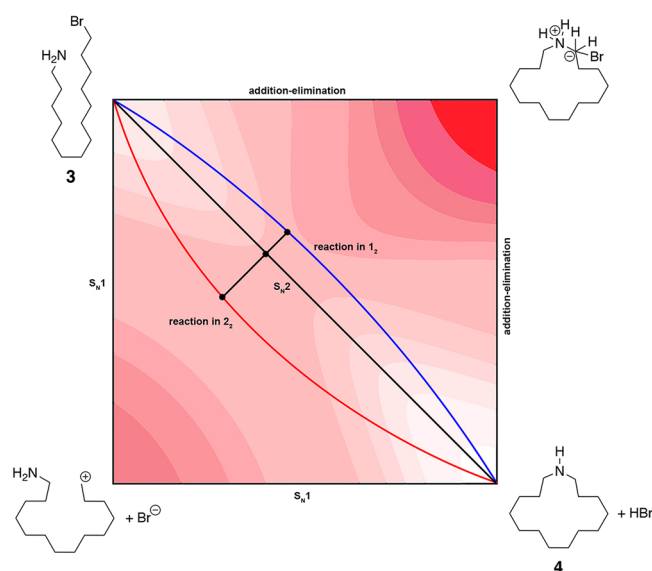
Figure 3. Representative More O'Ferrall–Jencks diagram illustrating the effects upon the cyclization of 14-bromotetradecan-1-amine (**3**) within the inner-spaces of positively and negatively charged capsules **1₂** and **2₂**. The black diagonal from top left to bottom right corresponds to the reaction coordinate of the idealized S_N2 mechanism. The left and lower axes correspond to the reaction coordinate of the idealized S_N1 mechanism, and top and right axes correspond to the reaction coordinate of an addition–elimination process involving a pentavalent carbanionic TS. The blue and red curves correspond to the enforced mechanisms within the inner-spaces of positively and negatively charged capsules **1₂** and **2₂**.

coordinate because of the overall exergonic nature of the cyclization (Hammond postulate). When the reaction is carried out in the negative EPF of capsule **2₂**, the reaction coordinate (red) is pulled toward the lower left as the field of the host enforces a mechanism involving the development of a greater degree of carbocation character in the TS. Compared to the idealized S_N2 mechanism, the activated complex and TS involve relatively long N···C and C···Br distances. In other words, capsule **2₂** behaves as the supramolecular equivalent of a typical (covalently attached) electron donating group

(EDG), with the EPF influencing electron distributions in the TS in a manner similar to the orbital effects arising from electronegativity differences between covalently attached EDGs. In contrast, within the positive EPF of capsule **1₂**, the reaction coordinate (blue) is curved toward the upper right as the field of the host enforces the development of a greater degree of carbanion character in the TS with relatively short N···C and C···Br distances. Thus, capsule **1₂** behaves as the supramolecular equivalent of an electron withdrawing group (EWG) on the reaction center. We show an asymmetry in the degree of deviation from the idealized S_N2 coordinate for the positive and negative capsules to reflect the idea that a trigonal bipyramidal (D_{3h}), hypervalent carbon represents a particularly high energy TS.[57−59]

To gain further insight into the cyclization of **3**, we opted to probe how the addition of excess (exogenous) salts affected the rate and activation thermodynamics of the reaction. As we discuss, studies of the effects of salts not only provide more insight into the reaction mechanism but also reveal the differences in solvation of the two capsules and how this affects reactions in the inner-space, as well as some of the limitations of these hosts as yoctoliter reaction flasks.

The Effects of Exogenous Salts on Cyclization. The effective charge of the two host capsules is less than their formal ±16 because of attenuation from associating counterions, and charge transfer to the solvation shell waters. Regarding ion association, we have previously demonstrated both specific ion binding to the crown of four ammonium groups defined by the pendent groups in **1**,[60] as well as nonspecific association (ion condensation) to the host and its dimer capsule.[41,61] In contrast, there are no specific cation binding sites in **2** or its capsule; only weak ion condensation has been observed.[41,62] Irrespective of the type of binding, increases in the ionic strength and/or swapping the capsule counterions by the addition of ions with higher cavitand affinity lead to a reduction in its EPF. In the case of the capsules, this can induce a change in the nature of an assembly[62] or modulate the chemical reactivity of an internalized guest.[42]

To gain more insight into the mechanism of the cyclization of **3** within the capsules, we investigated the effects on the
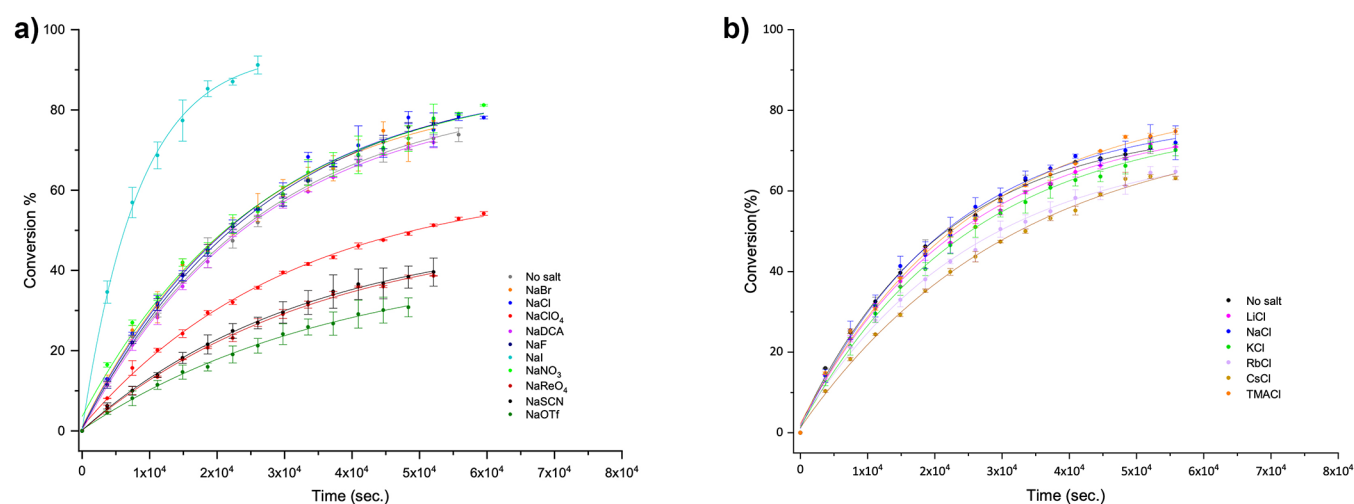
Figure 4. Plots of the conversion percentage as a function of time and salt for the formation of **4**. In both cases (a, b), the host-**3** complex concentration was 1 mM, and the total NaOD and/or salt concentration was 10 mM. For the effects of anions on the formation of **4** inside **1₂** (a), the reaction was carried out at 339 ± 1 K. For the effects of cations on the formation of **4** inside **2₂** (b), the cyclization temperature was 336 ± 1 K.

nature of exogenous salts upon reaction rates within the two hosts (SI, Section 5). To minimize pairing between the ions of the added salt, we selected highly solvated sodium and chloride counterions for, respectively, studying how anions and cations affect cyclization rates within 1_2 and within 2_2.[61,62] In all cases, the rate constants for cyclization were measured in the presence of 10 mM added salt and compared to the rate of the reaction with only base (NaOD) present. In most cases, ^{1}H NMR spectroscopy revealed that the added salt had no direct effect on the bound guest. However, in the presence of anions that bind strongly to the pocket of host **2**, namely, TfO$^-$, ReO$_4^-$, ClO$_4^-$, and SCN$^-$,[60] the bound guest region of the ^{1}H NMR spectrum did undergo small changes indicative of an alteration of the guest ingression–egression kinetics, and/or partial guest displacement by anion competition (see below).

Figure 4a shows how anion association to the outside of 1_2 affects the formation of **4**, while Table 2 presents the

Table 2. Reaction Rate Constant (k) for the Cyclization of 3 in 1_2 or 2_2 in the Presence of Different Salts[a]

Na$^+$ salt	rate constant,[b] k in 10^{-5} s^{-1}	Cl$^-$ salt	rate constant,[c] k in 10^{-5} s^{-1}
I$^-$	12.00	no salt	4.81
Br$^-$	4.07	Na$^+$	4.61
Cl$^-$	3.91	Li$^+$	4.26
CHCl$_2$CO$_2^-$	3.83	K$^+$	3.97
no salt	3.80	N(Me$_4$)$^+$	3.92
NO$_3^-$	3.76	Rb$^+$	3.88
F$^-$	3.69	Cs$^+$	3.15
ClO$_4^-$	3.25		
SCN$^-$	2.98		
ReO$_4^-$	2.86		
TfO$^-$	2.62		

[a]Errors in individual rate constant determinations <10%. [b]At 339 ± 1 K. [c]At 336 ± 1 K.

corresponding rate constant data. Iodide is the outlier here, accelerating the reaction considerably; all other anions either have little effect or reduced the rate constant. Iodide is known to enter the inner-space via capsule breathing, the microsecond time scale, the partial opening of the complex that allows the entry, and the exit of small solutes without allowing principal guest egression.[35,63,64] Thus, we believe that in the presence of NaI there are two sequential reactions occurring within 1_2: halogen exchange to form the corresponding iodinated guest, and then cyclization. Iodide is known to associate with the outside of **1** and its capsule,[60] so a rate attenuation mechanism (see below) is also likely to be in operation. However, this is evidently small compared to the increased cyclization rate arising from the *in situ* iodination.

The other anions either had little effect on the rate constant or caused its reduction. Reaction rate constants in the presence of strongly solvated F$^-$, Cl$^-$, Br$^-$, and NO$_3^-$, and amphiphilic CHCl$_2$CO$_2^-$, were very similar to salt free conditions. These have been shown to be the weakest of binders to the outside of **1**,[60] so this finding is not unexpected. In contrast, stronger binding, charge diffusion and weakly solvated SCN$^-$, ClO$_4^-$, ReO$_4^-$, and TfO$^-$ all attenuated cyclization rates. In these cases, extrapolation of the data indicated low yields of **4** in the region of 50–70%, suggesting that anion competition for the inner-space of the capsule (see above) leads to leakage of guest **3** and its ultimate polymerization or hydrolysis in free solution.

Figure 4b shows the raw conversion data as a function of time and cation for the cyclization of **3** within 2_2, while Table 2 summarizes the obtained rate constants. In general, the effect of alkali metal cations on the cyclization of **3** within 2_2 was found to be considerably smaller than the anion effect with 1_2 (Figure 4). This result is consistent with the high solvation free energy of carboxylate groups; capsule 2_2 cannot pair strongly with its counterions.

As with the anion effect on 1_2, all cations were observed to reduce the rate of cyclization inside 2_2. Although the effects of Na$^+$ or Li$^+$ were not significant, and in many cases differences between two salts were similar, a distinct trend was observed in which the larger and more polarizable cations attenuated cyclization more. Thus, the ability to attenuate the reaction was as follows: Cs$^+$ > Rb$^+$ > K$^+$ > Li$^+$ ≈ Na$^+$ ≈ no salt. This trend was very similar to the ability of cations to reduce the net charge of the host and switch a dimeric capsule into a tetrameric cavitand assembly.[62] Thus, contrary to Collins' law of matching water affinities which predicts sodium ions pairing most strongly with carboxylates,[65] by both the metrics of assembly switching and reaction attenuation, it is the larger, more weakly solvated cations that pair most strongly with the capsule. That noted, in addition to Coulombic interactions, cation–π interactions and other such ion–pole interactions may also be involved in the weak association of the cations with the outside of the cavity.

Figure 4 and Table 2 reveal that the attenuation of the EPF of either capsule increases the $\Delta G^{\ddagger}$ for cyclization of **3**. In other words, irrespective of whether a capsule enforces a mechanism that involves a TS with some degree or carbocation or carbanion character relative to the idealized S$_N$2 process, attenuation of the EPF slows the reaction. Why is this? Our working hypothesis is that in each capsule, the energetic cost of charge development in the activated complex and TS is attenuated by guest realignment to maximize favorable interactions between the guest and capsule. As a result, the corresponding cyclization within the confines of a capsule with little or no EPF is more energetically demanding. In other words, in free solution, solvent can transfer charge and/or hydrogen bond with the attacking N atom or the departing Br$^-$ group, but in a capsule devoid of any EPF and any groups that function as a formal proton shuttle or halide transporter, the S$_N$2 process is energetically demanding. This hypothesis dovetails well with the general observation that S$_N$2 processes involving charged species are slower in solvents of lower polarity.

For further information, we selected two of the afore-mentioned salts and carried out Eyring analyses to determine how ion association to the outside of a capsule affected the thermodynamics of TS formation. Specifically, we selected NaClO$_4$ to probe the effects of ClO$_4^-$, on the cyclization of **3** within 1_2, and CsCl to examine how Cs$^+$ condensation to 2_2 affected the reaction. Table 3 summarizes our findings. Briefly, attenuation of the EPF of both capsules leads to a rise in the enthalpy of activation. This rise is much larger in 1_2 ($\Delta\Delta H^{\ddagger}$ = 23.8 kJ mol^{-1} versus 5.9 kJ mol^{-1} in 2_2) indicating that increased counterion affinity to 1_2 leads to a greater EPF attenuation in this capsule. It was not possible to add more NaClO$_4$ without salting out of the complex. This, combined with the $\Delta H^{\ddagger}$ values for the reaction in both capsules in the presence of their respective salts being in the region of 80–90 kJ mol^{-1}, suggests a value in this region for reaction in the theoretical neutral host. Interestingly, the $-T\Delta S^{\ddagger}$ values in the

Table 3. Eyring Data for the Cyclization of Guest 3 within Capsules 1_2 and 2_2 in the Presence of 10 mM Added Salt

	3 in 1_2 + NaClO$_4$	3 in 2_2 + CsCl
k (s^{-1}, 338 K)	3.11×10^{-5}	3.83×10^{-5}
k (s^{-1}, 298.15 K)	5.15×10^{-7}	7.40×10^{-7}
half-life (s, 338 K)[a]	2.20×10^4	1.80×10^4
half-life (s, 298.15 K)[a]	1.34×10^6	9.36×10^5
$\Delta G^{\ddagger}$ (kJ mol^{-1})	108.9	107.6
$\Delta H^{\ddagger}$ (kJ mol^{-1})	83.6	80.4
$-T\Delta S^{\ddagger}$ (kJ mol^{-1})	25.3	27.3

[a]Errors in individual rate constant determinations <10%. Error in Eyring analysis ($\Delta G^{\ddagger}$, $-\Delta H^{\ddagger}$, $T\Delta S^{\ddagger}$) 5%.

two EPF-attenuated capsules are also very similar, leading to similar overall $\Delta G^{\ddagger}$ values. However, the bound guest ^{1}H NMR signal broadening and shifting in the presence of NaClO$_4$ means that it is not possible to determine if the two complexes have similar guest motifs when the charges on the host are largely removed.

CONCLUSIONS

Our results described here continue our investigation into the ability of capsules driven by the hydrophobic effect to function as yoctoliter reaction vessels. Our data reveals that both hosts can lead to essentially quantitative formation of cyclic amine **4**, and that relative to a theoretical charge neutral host, the reactions are promoted by both the positive EPF and the negative EPF of 1_2 and 2_2. We interpret this finding in terms of the EPF of each host being capable of stabilizing charge buildup in the activated complex and TS, but that each does so by enforcing different mechanisms from the idealized S$_N$2 process. Moreover, we conclude that the S$_N$2 mechanism in the theoretical neutral host devoid of an EPF is energetically demanding because of a lack of solvation in the inner-space of the capsule.

Our data also reveals that there is more control of the EPF in capsule 1_2 because it is more poorly hydrated and water-solubilizing, and charge groups pair more strongly with counterions. However, there is a limit here. Relatively high affinity, charge-diffuse anions can compete with **3** for the inner-space of the capsule and, as a result, attenuate the yield of product **4**. Conversely, maximal EPFs can be generated in solutions of low ionic strength using strongly solvated counterions that pair minimally with the capsule. We are continuing to study these assemblies as yoctoliter reaction flasks and will report our findings in due course.

ASSOCIATED CONTENT

Supporting Information

The Supporting Information is available free of charge at https://pubs.org/doi/10.1021/acs.jpcb.1c05238.

> Details of the synthesis of guest **3**, the guest encapsulation protocols, and a summary of the kinetic experiments and data analysis (PDF)

AUTHOR INFORMATION

Corresponding Author

Bruce C. Gibb − *Department of Chemistry, Tulane University, New Orleans, Louisiana 70118, United States;* orcid.org/0000-0002-4478-4084; Email: bgibb@tulane.edu

Authors

Wei Yao − *Department of Chemistry, Tulane University, New Orleans, Louisiana 70118, United States*

Kaiyu Wang − *Department of Chemistry, Tulane University, New Orleans, Louisiana 70118, United States*

Yahya A. Ismaiel − *Department of Chemistry, Tulane University, New Orleans, Louisiana 70118, United States*

Ruiqing Wang − *Department of Chemistry, Tulane University, New Orleans, Louisiana 70118, United States*

Xiaoyang Cai − *Department of Chemistry, Tulane University, New Orleans, Louisiana 70118, United States*

Mary Teeler − *Department of Chemistry, Tulane University, New Orleans, Louisiana 70118, United States*

Complete contact information is available at:
https://pubs.acs.org/10.1021/acs.jpcb.1c05238

Notes

The authors declare no competing financial interest.

REFERENCES

(1) Fried, S. D.; Boxer, S. G. Electric Fields and Enzyme Catalysis. *Annu. Rev. Biochem.* **2017**, *86* (1), 387−415.

(2) Fried, S. D.; Boxer, S. G. Measuring Electric Fields and Noncovalent Interactions Using the Vibrational Stark Effect. *Acc. Chem. Res.* **2015**, *48* (4), 998−1006.

(3) Petsko, G. A.; Ringe, D. *Protein Structure and Function*; New Science Press: Sunderland, MA, 2004.

(4) Zhang, X.; Houk, K. N. Why Enzymes are Proficient Catalysts: Beyond the Pauling Paradigm. *Acc. Chem. Res.* **2005**, *38*, 379−385.

(5) Warshel, A.; Sharma, P. K.; Kato, M.; Xiang, Y.; Liu, H.; Olsson, M. H. Electrostatic basis for enzyme catalysis. *Chem. Rev.* **2006**, *106* (8), 3210−35.

(6) Wolfenden, R. Degrees of Difficulty of Water-Consuming Reactions in the Absence of Enzymes. *Chem. Rev.* **2006**, *106* (8), 3379−3396.

(7) Zare, R. The quest to control chemical reactions using interfacial electric fields. *Chemistry World* **2020**, No. October, 23.

(8) Chamberlayne, C. F.; Zare, R. N. Simple model for the electric field and spatial distribution of ions in a microdroplet. *J. Chem. Phys.* **2020**, *152* (18), 184702.

(9) Aragones, A. C.; Haworth, N. L.; Darwish, N.; Ciampi, S.; Bloomfield, N. J.; Wallace, G. G.; Diez-Perez, I.; Coote, M. L. Electrostatic catalysis of a Diels-Alder reaction. *Nature* **2016**, *531* (7592), 88−91.

(10) Zhao, A.; Tan, S.; Li, B.; Wang, B.; Yang, J.; Hou, J. G. STM tip-assisted single molecule chemistry. *Phys. Chem. Chem. Phys.* **2013**, *15* (30), 12428−12441.

(11) Alemani, M.; Peters, M. V.; Hecht, S.; Rieder, K.-H.; Moresco, F.; Grill, L. Electric Field-Induced Isomerization of Azobenzene by STM. *J. Am. Chem. Soc.* **2006**, *128* (45), 14446−14447.

(12) Hla, S.-W.; Rieder, K.-H. STM Control of Chemical Reactions: Single-Molecule Synthesis. *Annu. Rev. Phys. Chem.* **2003**, *54* (1), 307−330.

(13) Shi, M. W.; Thomas, S. P.; Hathwar, V. R.; Edwards, A. J.; Piltz, R. O.; Jayatilaka, D.; Koutsantonis, G. A.; Overgaard, J.; Nishibori, E.; Iversen, B. B.; Spackman, M. A. Measurement of Electric Fields Experienced by Urea Guest Molecules in the 18-Crown-6/Urea (1:5) Host−Guest Complex: An Experimental Reference Point for Electric-Field-Assisted Catalysis. *J. Am. Chem. Soc.* **2019**, *141* (9), 3965−3976.

(14) Spackman, P. R.; Yu, L.-J.; Morton, C. J.; Parker, M. W.; Bond, C. S.; Spackman, M. A.; Jayatilaka, D.; Thomas, S. P. Bridging Crystal

Engineering and Drug Discovery by Utilizing Intermolecular Interactions and Molecular Shapes in Crystals. *Angew. Chem., Int. Ed.* **2019**, *58* (47), 16780−16784.

(15) Shaik, S.; Mandal, D.; Ramanan, R. Oriented electric fields as future smart reagents in chemistry. *Nat. Chem.* **2016**, *8* (12), 1091−1098.

(16) Pocker, Y.; Buchholz, R. F. Electrostatic catalysis by ionic aggregates. II. Reversible elimination of hydrogen chloride from tert-butyl chloride and the rearrangement of 1-phenylallyl chloride in lithium perchlorate-diethyl ether solutions. *J. Am. Chem. Soc.* **1970**, *92* (13), 4033−4038.

(17) Brown, C. J.; Toste, F. D.; Bergman, R. G.; Raymond, K. N. Supramolecular catalysis in metal-ligand cluster hosts. *Chem. Rev.* **2015**, *115* (9), 3012−35.

(18) Yoshizawa, M.; Klosterman, J. K.; Fujita, M. Functional Molecular Flasks: New Properties and Reactions within Discrete, Self-Assembled Hosts. *Angew. Chem., Int. Ed.* **2009**, *48*, 3418−3438.

(19) Assaf, K. I.; Nau, W. M. Cucurbiturils: from synthesis to high-affinity binding and catalysis. *Chem. Soc. Rev.* **2015**, *44* (2), 394−418.

(20) Meeuwissen, J.; Reek, J. N. Supramolecular catalysis beyond enzyme mimics. *Nat. Chem.* **2010**, *2* (8), 615−21.

(21) Mosca, S.; Yu, Y.; Gavette, J. V.; Zhang, K. D.; Rebek, J., Jr. A Deep Cavitand Templates Lactam Formation in Water. *J. Am. Chem. Soc.* **2015**, *137* (46), 14582−5.

(22) Masseroni, D.; Mosca, S.; Mower, M. P.; Blackmond, D. G.; Rebek, J., Jr. Cavitands as Reaction Vessels and Blocking Groups for Selective Reactions in Water. *Angew. Chem., Int. Ed.* **2016**, *55* (29), 8290−3.

(23) Horiuchi, S.; Nishioka, Y.; Murase, T.; Fujita, M. Both [2 + 2] and [2 + 4] additions of inert aromatics via identical ternary host−guest complexes. *Chem. Commun.* **2010**, *46*, 3460−3462.

(24) Murase, T.; Horiuchi, S.; Fujita, M. Naphthalene Diels-Alder in a Self-Assembled Molecular Flask. *J. Am. Chem. Soc.* **2010**, *132*, 2866−2867.

(25) Hong, C. M.; Kaphan, D. M.; Bergman, R. G.; Raymond, K. N.; Toste, F. D. Conformational Selection as the Mechanism of Guest Binding in a Flexible Supramolecular Host. *J. Am. Chem. Soc.* **2017**, *139* (23), 8013−8021.

(26) Kaphan, D. M.; Levin, M. D.; Bergman, R. G.; Raymond, K. N.; Toste, F. D. A supramolecular microenvironment strategy for transition metal catalysis. *Science* **2015**, *350*, 1235−1238.

(27) Yoshizawa, M.; Tamura, M.; Fujita, M. Diels-Alder in Aqueous Molecular Hosts: Unusual Regioselectivity and Efficient Catalysis. *Science* **2006**, *312*, 251−254.

(28) Cullen, W.; Misuraca, M. C.; Hunter, C. A.; Williams, N. H.; Ward, M. D. Highly efficient catalysis of the Kemp elimination in the cavity of a cubic coordination cage. *Nat. Chem.* **2016**, *8* (3), 231−6.

(29) Shi, Q.; Mower, M. P.; Blackmond, D. G.; Rebek, J., Jr. Water-soluble cavitands promote hydrolyses of long-chain diesters. *Proc. Natl. Acad. Sci. U. S. A.* **2016**, *113* (33), 9199−203.

(30) Zhang, Q.; Catti, L.; Kaila, V. R. I.; Tiefenbacher, K. To catalyze or not to catalyze: elucidation of the subtle differences between the hexameric capsules of pyrogallolarene and resorcinarene. *Chem. Sci.* **2017**, *8*, 1653−1657.

(31) Zhang, Q.; Tiefenbacher, K. Terpene cyclization catalysed inside a self-assembled cavity. *Nat. Chem.* **2015**, *7* (3), 197−202.

(32) Zhang, Q.; Tiefenbacher, K. Hexameric Resorcinarene Capsule is a Bronsted Acid: Investigation and Application to Synthesis and Catalysis. *J. Am. Chem. Soc.* **2013**, *135* (43), 16213−9.

(33) Kaanumalle, L. S.; Gibb, C. L. D.; Gibb, B. C.; Ramamurthy, V. Controlling Photochemistry with Distinct Hydrophobic Nanoenvironments. *J. Am. Chem. Soc.* **2004**, *126* (44), 14366−14367.

(34) Kaanumalle, L. S.; Gibb, C. L. D.; Gibb, B. C.; Ramamurthy, V. A Hydrophobic Nanocapsule Controls the Photophysics of Aromatic Molecules by Suppressing Their Favored Solution Pathways. *J. Am. Chem. Soc.* **2005**, *127* (11), 3674−3675.

(35) Natarajan, A.; Kaanumalle, L. S.; Jockusch, S.; Gibb, C. L. D.; Gibb, B. C.; Turro, N. J.; Ramamurthy, V. Controlling Photoreactions with Restricted Spaces and Weak Intermolecular Forces: Remarkable

(36) Gibb, C. L. D.; Sundaresan, A. K.; Ramamurthy, V.; Gibb, B. C. Templation of the Excited-State Chemistry of α-(n-Alkyl) Dibenzyl Ketones: How Guest Packing within a Nanoscale Supramolecular Capsule Influences Photochemistry. *J. Am. Chem. Soc.* **2008**, *130* (12), 4069−4080.

(37) For an important exception, see: Hong, C. M.; Morimoto, M.; Kapustin, E. A.; Alzakhem, N.; Bergman, R. G.; Raymond, K. N.; Toste, F. D. Deconvoluting the Role of Charge in a Supramolecular Catalyst. *J. Am. Chem. Soc.* **2018**, *140* (21), 6591−6595.

(38) Gibb, C. L. D.; Gibb, B. C. Well Defined, Organic Nano-Environments in Water: The Hydrophobic Effect Drives a Capsular Assembly. *J. Am. Chem. Soc.* **2004**, *126*, 11408−11409.

(39) Liu, S.; Whisenhunt-Ioup, S. E.; Gibb, C. L. D.; Gibb, B. C. An improved synthesis of 'octa-acid' deep-cavity cavitand. *Supramol. Chem.* **2011**, *23* (6), 480−485.

(40) Hillyer, M. B.; Gibb, C. L. D.; Sokkalingam, P.; Jordan, J. H.; Ioup, S. E.; Gibb, B. C. Synthesis of Water-Soluble Deep-Cavity Cavitands. *Org. Lett.* **2016**, *18* (16), 4048−51.

(41) Cai, X.; Kataria, R.; Gibb, B. C. Intrinsic and Extrinsic Control of the pK_a of Thiol Guests inside Yoctoliter Containers. *J. Am. Chem. Soc.* **2020**, *142* (18), 8291−8298.

(42) Wang, K.; Cai, X.; Yao, W.; Tang, D.; Kataria, R.; Ashbaugh, H. S.; Byers, L. D.; Gibb, B. C. Electrostatic Control of Macrocyclization Reactions within Nanospaces. *J. Am. Chem. Soc.* **2019**, *141*, 6740−6747.

(43) Barnett, J. W.; Gibb, B. C.; Ashbaugh, H. S. Succession of Alkane Conformational Motifs Bound within Hydrophobic Supramolecular Capsular Assemblies. *J. Phys. Chem. B* **2016**, *120* (39), 10394−10402.

(44) Wang, K.; Gibb, B. C. Mapping the Binding Motifs of Deprotonated Monounsaturated Fatty Acids and Their Corresponding Methyl Esters within Supramolecular Capsules. *J. Org. Chem.* **2017**, *82*, 4279−4288.

(45) Zhang, K. D.; Ajami, D.; Gavette, J. V.; Rebek, J., Jr. Alkyl groups fold to fit within a water-soluble cavitand. *J. Am. Chem. Soc.* **2014**, *136* (14), 5264−6.

(46) Choudhury, R.; Barman, A.; Prabhakar, R.; Ramamurthy, V. Hydrocarbons depending on the chain length and head group adopt different conformations within a water-soluble nanocapsule: 1H NMR and molecular dynamics studies. *J. Phys. Chem. B* **2013**, *117* (1), 398−407.

(47) Liu, S.; Russell, D. H.; Zinnel, N. F.; Gibb, B. C. Guest packing motifs within a supramolecular nanocapsule and a covalent analogue. *J. Am. Chem. Soc.* **2013**, *135* (11), 4314−24.

(48) Asadi, A.; Ajami, D.; Rebek, J., Jr. Bent alkanes in a new thiourea-containing capsule. *J. Am. Chem. Soc.* **2011**, *133* (28), 10682−4.

(49) Ko, Y. H.; Kim, H.; Kim, Y.; Kim, K. U-shaped Conformation of Alkyl Chains Bound to a Synthetic Host. *Angew. Chem., Int. Ed.* **2008**, *47*, 4106−4109.

(50) Marcus, Y. *Ion Properties*, 1st ed.; Marcel Dekker: New York, 1997.

(51) Shi, Q.; Masseroni, D.; Rebek, J., Jr. Macrocyclization of Folded Diamines in Cavitands. *J. Am. Chem. Soc.* **2016**, *138*, 10846.

(52) Wu, N. W.; Rebek, J., Jr. Cavitands as Chaperones for Monofunctional and Ring-Forming Reactions in Water. *J. Am. Chem. Soc.* **2016**, *138* (24), 7512−5.

(53) Yang, J. M.; Yu, Y.; Rebek, J., Jr. Selective Macrocycle Formation in Cavitands. *J. Am. Chem. Soc.* **2021**, *143*, 2190.

(54) In these experiments, we assumed that any trace protonation of the amine guest inside the negatively charged capsule did not significantly affect the Eyring analysis.

(55) Jencks, W. P. A primer for the Bema Hapothle. An empirical approach to the characterization of changing transition-state structures. *Chem. Rev.* **1985**, *85* (6), 511−527.

(56) Anslyn, E. V.; Dougherty, D. A. *Modern Physical Organic Chemistry*; University Science Books: Sausalito, 2006.

(57) Pierrefixe, S. C. A. H.; Fonseca Guerra, C.; Bickelhaupt, F. M. Hypervalent Silicon versus Carbon: Ball-in-a-Box Model. *Chem. - Eur. J.* **2008**, *14* (3), 819−828.

(58) Pierrefixe, S. C.; van Stralen, S. J.; van Stralen, J. N.; Fonseca Guerra, C.; Bickelhaupt, F. M. Hypervalent carbon atom: "freezing" the S(N)2 transition state. *Angew. Chem., Int. Ed.* **2009**, *48* (35), 6469−71.

(59) Olmstead, W. N.; Brauman, J. I. Gas-phase nucleophilic displacement reactions. *J. Am. Chem. Soc.* **1977**, *99* (13), 4219−4228.

(60) Jordan, J. H.; Gibb, C. L. D.; Wishard, A.; Pham, T.; Gibb, B. C. Ion-Hydrocarbon and/or Ion-Ion Interactions: Direct and Reverse Hofmeister Effects in a Synthetic Host. *J. Am. Chem. Soc.* **2018**, *140* (11), 4092−4099.

(61) Wishard, A.; Gibb, B. C. Dynamic light scattering studies of the effects of salts on the diffusivity of cationic and anionic cavitands. *Beilstein J. Org. Chem.* **2018**, *14*, 2212−2219.

(62) Hillyer, M. B.; Gan, H.; Gibb, B. C. Precision Switching in a Discrete Supramolecular Assembly: Alkali Metal Ion-Carboxylate Selectivities and the Cationic Hofmeister Effect. *ChemPhysChem* **2018**, *19* (18), 2285−2289.

(63) Tang, H.; de Oliveira, C. S.; Sonntag, G.; Gibb, C. L.; Gibb, B. C.; Bohne, C. Dynamics of a supramolecular capsule assembly with pyrene. *J. Am. Chem. Soc.* **2012**, *134* (12), 5544−7.

(64) Jayaraj, N.; Jockusch, S.; Kaanumalle, L. S.; Turro, N. J.; Ramamurthy, V. Dynamics of capsuleplex formed between octaacid and organic guest molecules — Photophysical techniques reveal the opening and closing of capsuleplex. *Can. J. Chem.* **2011**, *89* (2), 203−213.

(65) Collins, K. D. Ion hydration: Implications for cellular function, polyelectrolytes, and protein crystallization. *Biophys. Chem.* **2006**, *119* (3), 271−281.